Properties of deformed nuclei in improved quark mass density-dependent model

Ren-li Xu (徐仁力)
(Department of Physics, Nanjing University)

Advisor: Zhong-Zhou Ren

outline

1. Introduction

2. Parametrization for improved quark mass density-dependent model on finite nuclei

3. Summary

1. Introduction

Improved quark mass dendity-dependent model (IQMDD)

$$L_Q = \overline{\varphi}[\gamma^\mu (i\partial_\mu - g_\omega^q \omega_\mu - \frac{g_\rho^q}{2}\tau\rho_\mu) - m_q + g_\sigma^q \sigma]\varphi + \frac{1}{2}\partial^\mu \sigma \partial_\mu \sigma - U(\sigma)$$
$$- \frac{1}{4}\Omega^{\mu\nu}\Omega_{\mu\nu} + \frac{1}{2} m_\omega^2 \omega^\mu \omega_\mu - \frac{1}{4} G^{\mu\nu} G_{\mu\nu} + \frac{1}{2} m_\rho^2 \rho^\mu \rho_\mu$$

$$U(\sigma) = \frac{1}{2} m_\sigma^2 \sigma^2 + \frac{1}{3} b\sigma^3 + \frac{1}{4} c\sigma^4 + B$$

The bag constant **B** is introduced so that

$$U(\sigma_v) = 0, \qquad U(0) = B.$$

Lagrangian density at the hadronic level under the MFA

The effective nucleon mass is obtained from the bag energy

$$M_N^* = \sum_q E_q = \sum_q \frac{4}{3}\pi R^3 \frac{\Gamma_q}{(2\pi)^3}\int_0^{K_F^q} \sqrt{m_q^{*2} + k^2}\,(\frac{dN_q}{dk})dk$$

The bag radius R can be determined by

$$\frac{\delta M_N^*}{\delta R} = 0$$

$$\begin{aligned} L_H = {} & \overline{\psi}[i\gamma^\mu \partial_\mu - M_N^*(\sigma) - g_\omega \gamma^0 \omega_0(\mathbf{r}) - \frac{g_\rho}{2}\gamma^0 \tau_3 \rho_0(\mathbf{r}) \\ & - \frac{e}{2}\gamma^0(1+\tau_3)A_0(\mathbf{r})]\psi - \frac{1}{2}[\nabla\sigma(\mathbf{r})]^2 - U(\sigma) + \frac{1}{2}\{[\nabla\omega_0(\mathbf{r})]^2 + m_\omega^2 \omega_0(\mathbf{r})^2\} \\ & + \frac{1}{2}\{[\nabla\rho_0(\mathbf{r})]^2 + m_\rho^2 \rho_0(\mathbf{r})^2\} + \frac{1}{2}[\nabla A_0(\mathbf{r})]^2 \end{aligned}$$

2. Parametrization for IQMDD model on finite nuclei

Binding energy & spin-orbit splittings of finite nuclei in IQMDD

Table 1
The binding energy (in MeV) for ^{16}O and ^{208}Pb with NL3, FSU and IQMDD.

Nucleus	Expt	NL3	FSU	IQMDD
^{16}O	127.62	128.62	127.36	131.36
^{208}Pb	1636.43	1639.04	1636.96	1547.52

C. Wu and R. K. Su, J. Phys. G: Nucl. Part. Phys. **36**, 095101 (2009)
C. Wu and Z. Z. Ren, J. Phys. G: Nucl. Part. Phys. **37**, 105110 (2010)

Binding energy & spin-orbit splittings of finite nuclei in IQMDD

Table 2

The spin-orbit spittings for ^{40}Ca and ^{208}Pb in IQMDD and RMF models (NL3, FSU) . All the quantities are in MeV.

Model	^{40}Ca		^{208}Pb	
	Proton	Neutron	Proton	Neutron
	$1d_{5/2}-1d_{3/2}$	$1d_{5/2}-1d_{3/2}$	$1g_{9/2}-1g_{7/2}$	$2f_{7/2}-2f_{5/2}$
NL3	-6.6	-6.7	-4.2	-2.0
FSU	-6.3	-6.3	-3.8	-2.0
IQMDD	-2.0	-2.6	-1.0	-0.6
Expt	-7.2	-6.3	-4.0	-1.8

Modified IQMDD model

$$L_T = \bar{\varphi} \frac{f_\omega g_\omega^q}{2M_N} \sigma^{\mu\nu} \partial_\nu \omega_\mu \varphi + \eta {g_\rho^q}^2 {g_\omega^q}^2 \omega_\mu \omega^\mu \rho_\mu \rho^\mu$$

Table 3

The parameter sets for IQMDD and IQMDD-2 models. The b, m_σ, m_ω and m_ρ are given in MeV. The bag constant is fix at B= 174.0 MeV fm-3 in both models.

Model	m_σ	m_ω	m_ρ	g_σ^q	${g_\omega^q}^2$	${g_\rho^q}^2$	b	f_ω	η
IQMDD	509	783	770	4.67	5.9536	82.2649	-1460	0	0
IQMDD-2	508	782.5	763	5.09	8.8780	97.2642	-3400	2.1	0.01

Spin-orbit splittings of finite nuclei in IQMDD-2

Table 4

The spin-orbit spittings for ^{40}Ca and ^{208}Pb in IQMDD and RMF models (NL3, FSU) . All the quantities are in MeV.

Model	^{40}Ca		^{208}Pb	
	Proton $1d_{5/2}-1d_{3/2}$	Neutron $1d_{5/2}-1d_{3/2}$	Proton $1g_{9/2}-1g_{7/2}$	Neutron $2f_{7/2}-2f_{5/2}$
NL3	-6.6	-6.7	-4.2	-2.0
FSU	-6.3	-6.3	-3.8	-2.0
IQMDD	-2.0	-2.6	-1.0	-0.6
IQMDD-2	-6.3	-6.3	-3.8	-2.1
Expt	-7.2	-6.3	-4.0	-1.8

R. L. Xu, C. Wu, Z. Z. Ren, S. Kumar, and J. Liu, Nucl. Phys. A **907**, 1 (2013)

Binding energies of finite nuclei in IQMDD-2

Table 5

The binding energy per nucleon, rms charge raii and the neutron skin thickness for ^{16}O, ^{40}Ca and ^{208}Pb with NL3, FSU, IQMDD and IQMDD-2.

Nucleus	Observable	Expt	NL3	FSU	IQMDD	IQMDD-2
^{16}O	B/A (MeV)	7.98	8.04	7.96	8.21	8.03
	Rch (fm)	2.70	2.71	2.70	2.70	2.72
	Rn-Rp (fm)	--	-0.03	-0.03	-0.03	-0.03
^{40}Ca	B/A (MeV)	8.55	8.54	8.54	8.52	8.54
	Rch (fm)	3.47	3.47	3.44	3.43	3.45
	Rn-Rp (fm)	--	-0.05	-0.05	-0.05	-0.05
^{208}Pb	B/A (MeV)	7.87	7.88	7.87	7.44	7.83
	Rch (fm)	5.50	5.51	5.52	5.53	5.50
	Rn-Rp (fm)	--	0.28	0.21	0.22	0.24

Binding energies of finite nuclei in IQMDD-2

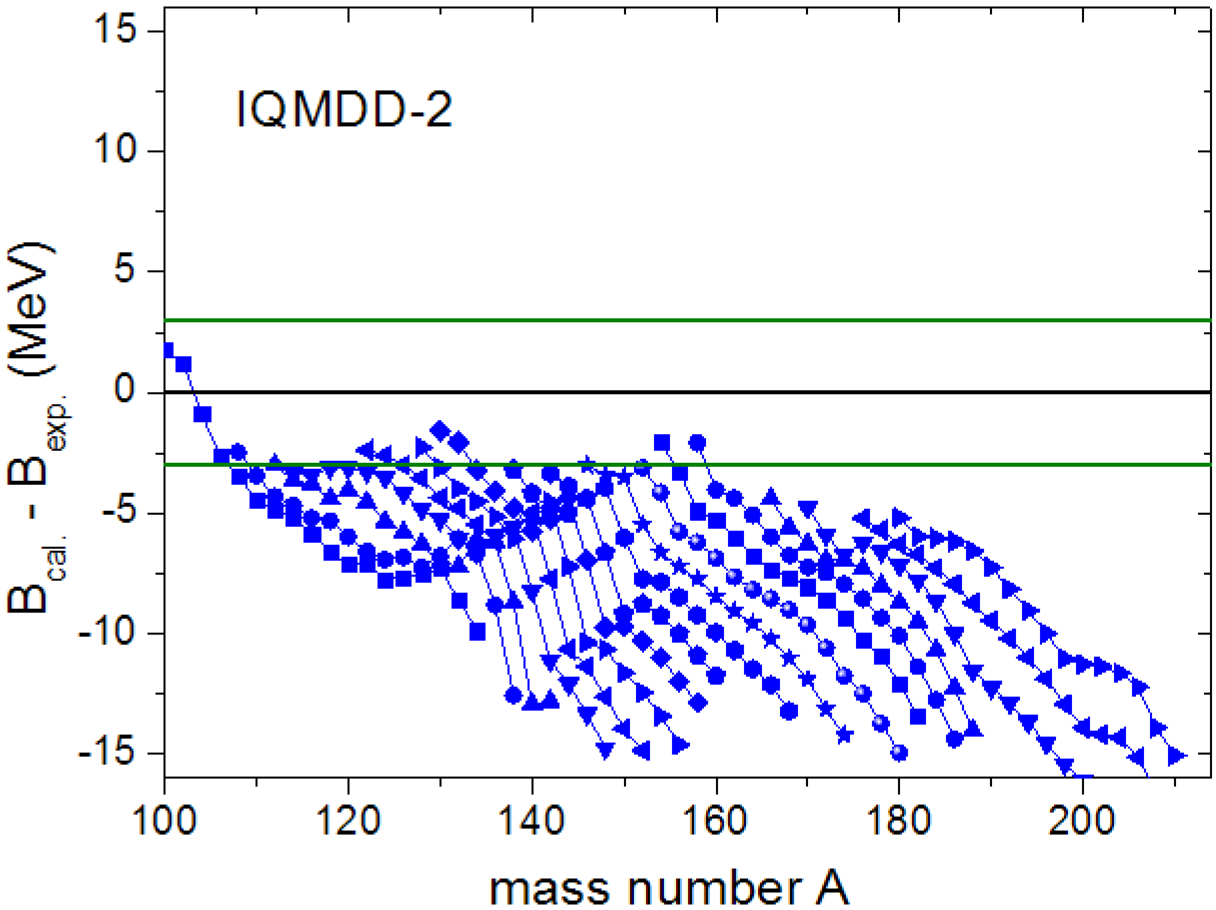

Fig. 1. Binding energy obtained in IQMDD-2. The calculated nuclei mainly range from Z=50 to Z=82

Modified IQMDD model

Table 6

The parameter sets for IQMDD-2 and IQMDD2* models. The b, m_σ , m_ω and m_ρ are given in MeV. The bag constant is fix at B= 174.0 MeV fm-3 in both models.

Model	m_σ	m_ω	m_ρ	g_σ^q	${g_\omega^q}^2$	${g_\rho^q}^2$	b	f_ω	η
IQMDD-2	508	782.5	763	5.09	8.8780	97.2642	-3400	2.1	0.01
IQMDD2*	508	782.5	763	5.09	8.8780	94.0914	-3400	2.1	0.03

Binding energies of finite nuclei in IQMDD2*

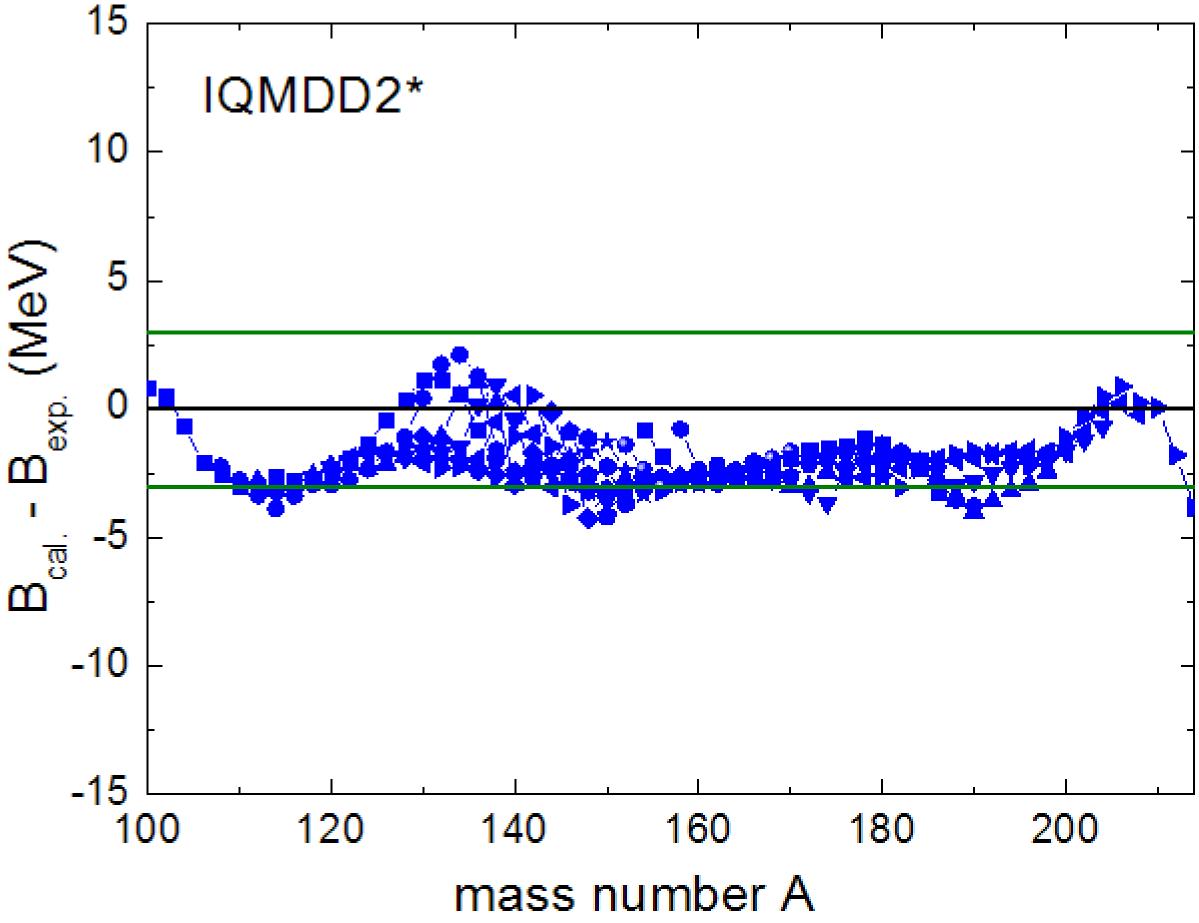

Fig. 2. Binding energy obtained in IQMDD2*. The calculated nuclei mainly range from Z=50 to Z=82

Quadrupole deformation of finite nuclei in IQMDD2*

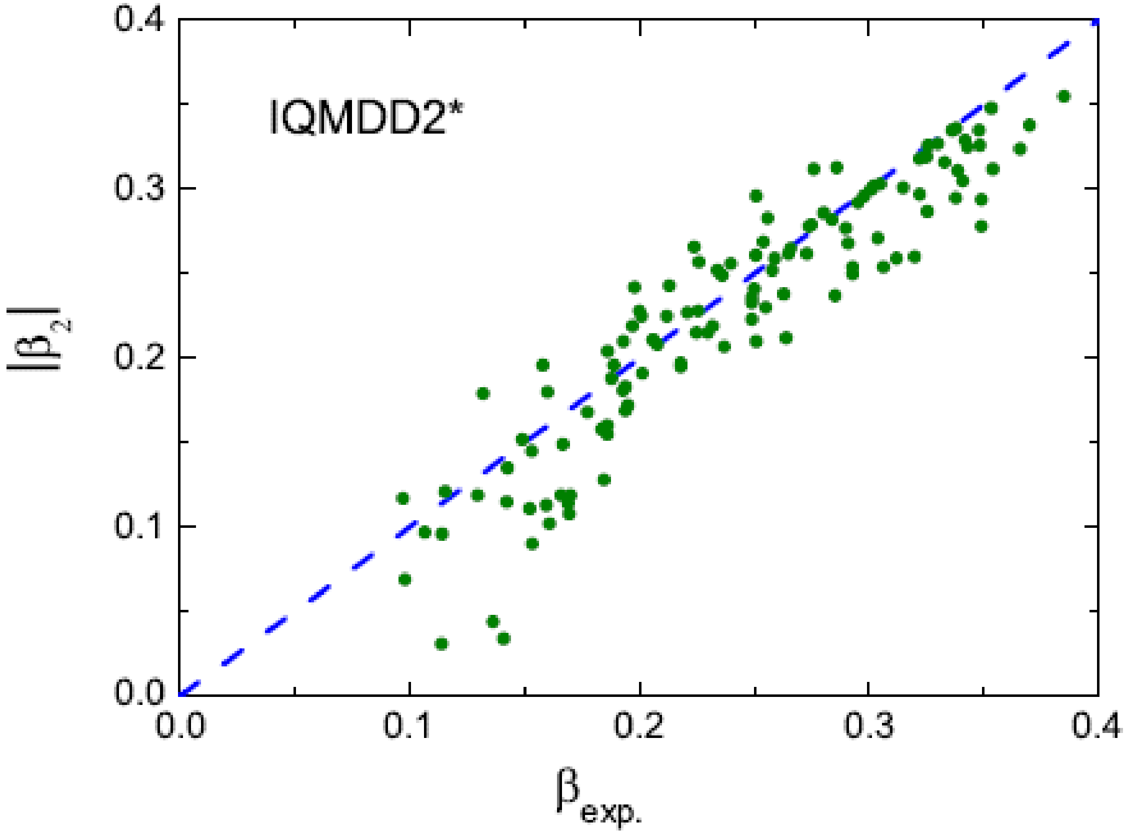

Fig. 3. The calculated absolute values of quadrupole deformation β_2 obtained by IQMDD2*.

Quadrupole deformation of finite nuclei in IQMDD2*

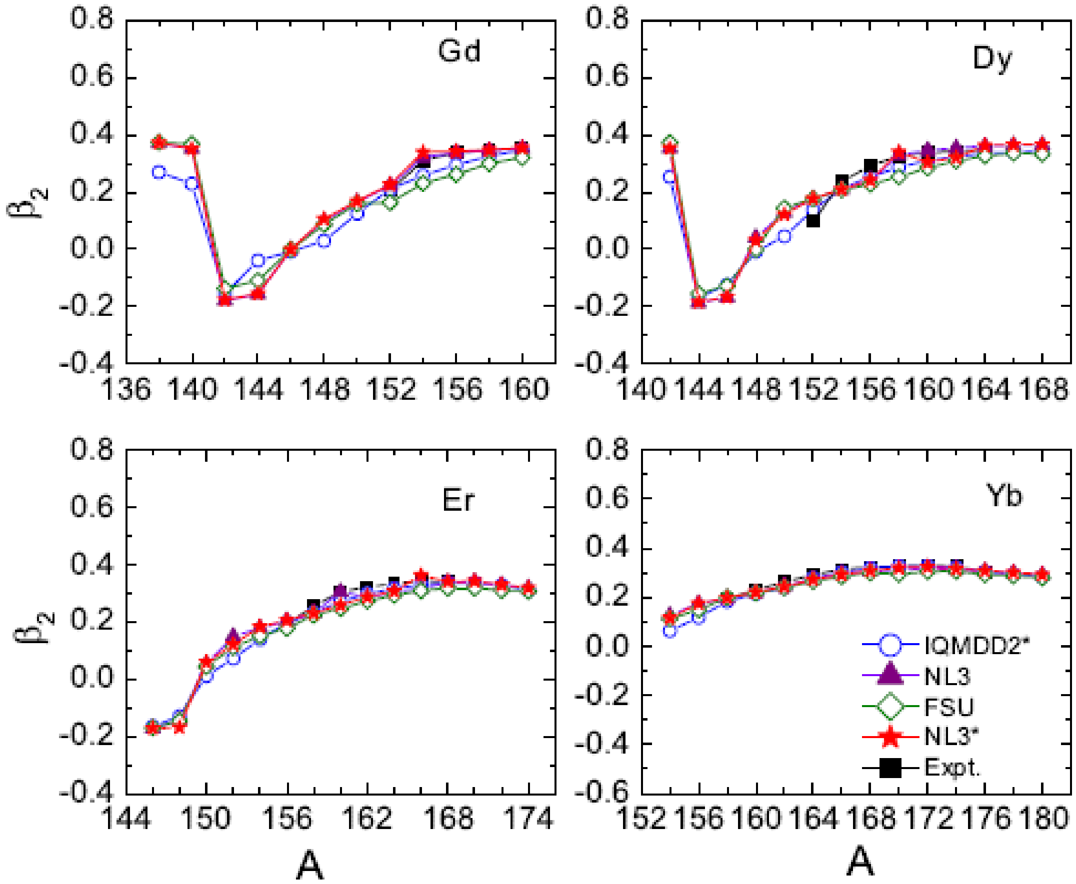

Fig. 4. The calculated values of quadrupole deformation β_2 for Gd, Dy, Er and Yb isotopic chains obtained by IQMDD2*, FSU, NL3 and NL3* respectively.

Summary

1. We have refitted the improved quark mass density-dependent model with the experimentally well-determined nuclear observables. The parameter set is refered to as IQMDD2*.

2. The IQMDD2* parameter set has been used to investigated the ground-state properties of deformed nuclei.

Thank you

Nucleus	Expt.		IQMDD2*			
	E/A	R_c	E/A	R_n	R_p	R_c
^{14}O	–7.05		–7.06	2.50	2.76	2.80
^{16}O	–7.98	2.70	–7.99	2.67	2.71	2.77
^{18}O	–7.77	2.77	–7.81	2.89	2.70	2.81
^{20}O	–7.57		–7.61	3.04	2.71	2.82
^{22}O	–7.36		–7.40	3.17	2.73	2.83
^{24}O	–7.04		–7.07	3.34	2.76	2.85
^{16}Ne	–6.08		–6.11	2.51	3.07	3.18
^{18}Ne	–7.34	2.97	–7.40	2.65	2.93	3.01
^{20}Ne	–8.03	3.01	–7.91	2.85	2.88	3.00
^{22}Ne	–8.08	2.95	–8.05	3.01	2.89	2.98
^{24}Ne	–7.99	2.90	–8.00	3.10	2.87	2.96
^{26}Ne	–7.75	2.93	–7.75	3.25	2.89	2.97
^{38}AR	–8.61	3.40	–8.59	3.35	3.32	3.41
^{40}AR	–8.60	3.43	–8.60	3.44	3.33	3.42
^{42}AR	–8.56	3.44	–8.56	3.52	3.35	3.43
^{44}AR	–8.49	3.45	–8.50	3.60	3.36	3.45
^{46}AR	–8.41	3.44	–8.40	3.67	3.38	3.46
^{48}AR	–8.24		–8.22	3.78	3.40	3.48
^{34}CA	–7.20		–7.20	3.10	3.44	3.54
^{36}CA	–7.82		–7.79	3.19	3.42	3.51
^{38}CA	–8.24		–8.21	3.28	3.41	3.50
^{40}CA	–8.55	3.48	–8.53	3.35	3.40	3.49

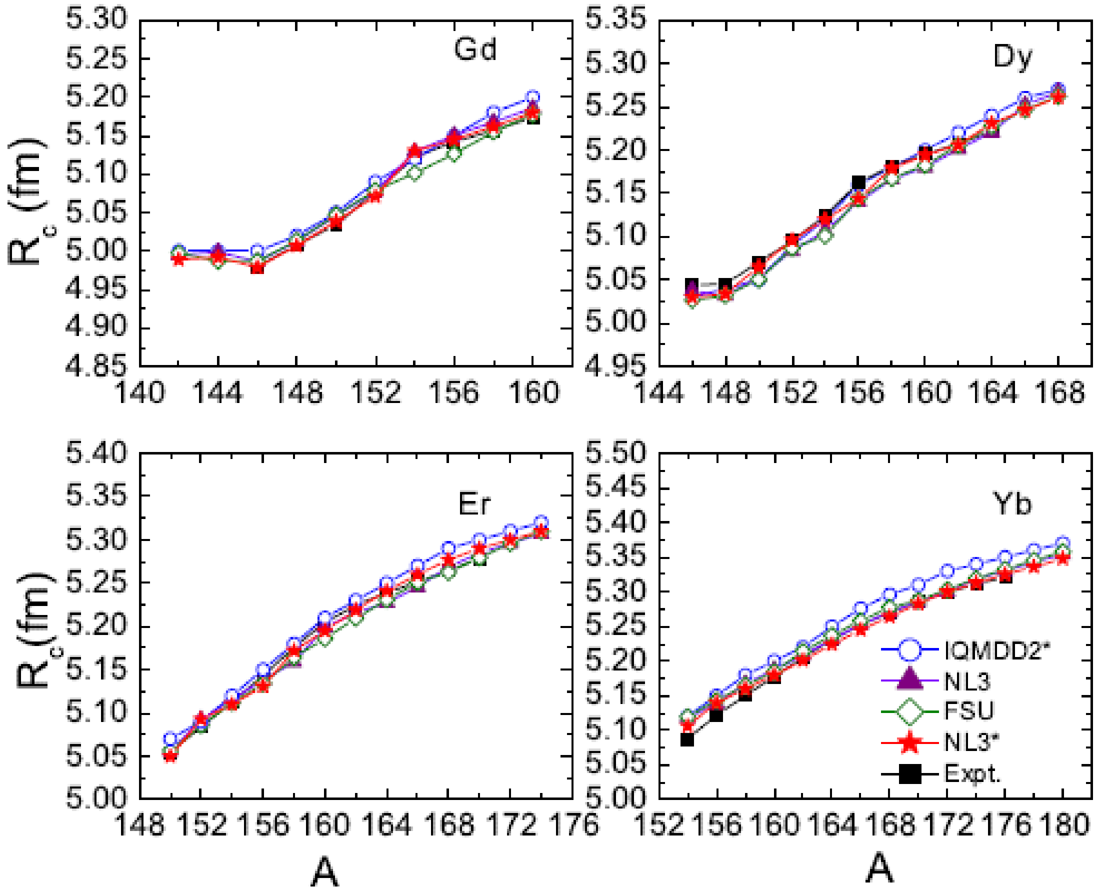

Fig. 6. The calculated charge radii R_c for Gd, Dy, Er and Yb isotopic chains by IQMDD2*, NL3, NL3* and FSU, together with the experimental data.

$$m_q = \frac{B}{3n_B} \quad (q = u, d, \bar{u}, \bar{d}), \tag{1}$$

$$m_{s,\bar{s}} = m_{s0} + \frac{B}{3n_B} \,. \tag{2}$$

$$m_q^* = m_q - g_\sigma^q \sigma.$$

$m_q \approx 150$ MeV

$$M_N^* = M_N - g_\sigma \sigma \,,$$

$$M_N^* = \sum_q E_q = \sum_q \frac{4}{3}\pi R^3 \frac{\Gamma_q}{(2\pi)^3} \int_0^{K_F^q} \sqrt{m_q^{*2} + k^2} \left(\frac{dN_q}{dk}\right) dk$$

$$\left[i\gamma^{\mu}\partial_{\mu} - M_N^* - g_{\omega}\gamma^0\omega_0(\mathbf{r}) - \frac{g_{\rho}}{2}\gamma^0\tau_3\rho_0(\mathbf{r}) \right.$$
$$\left. + \frac{f_{\omega}g_{\omega}}{2M_N}\sigma^{0i}\partial_i\omega_0(\mathbf{r}) - \frac{e}{2}\gamma^0(1+\tau_3)A_0(\mathbf{r})\right]\psi = 0.$$

$$(-\Delta + m_{\sigma}^2)\sigma(\mathbf{r}) = -\frac{\partial M_N^*}{\partial\sigma}\rho_s(\mathbf{r}) - b\sigma^2(\mathbf{r}) - c\sigma^3(\mathbf{r}),$$
$$(-\Delta + m_{\omega}^2)\omega_0(\mathbf{r}) = g_{\omega}\rho_v(\mathbf{r}) + \frac{f_{\omega}g_{\omega}}{2M_N}\rho_0^T(r)$$
$$-2\eta g_{\rho}^2 g_{\omega}^2\rho_0^2(r)\omega_0(r),$$
$$(-\Delta + m_{\rho}^2)\rho_0(\mathbf{r}) = \frac{g_{\rho}}{2}\rho_3(\mathbf{r}) - 2\eta g_{\rho}^2 g_{\omega}^2\rho_0(r)\omega_0^2(r),$$
$$-\Delta A_0(\mathbf{r}) = e\rho_p(\mathbf{r}),$$